2015 International Symposium on Nonlinear Theory and its Applications
NOLTA2015, Kowloon, Hong Kong, China, December 1-4, 2015

Synchronization of Piecewise-Constant Oscillators with Master-Slave Coupling

Yuya Sekine† and Tadashi Tsubone‡

†Nagaoka University of Technology
1603-1, Kamitomioka, Nagaoka, Niigata, 940-2188, Japan
Email: s123142@stn.nagaokaut.ac.jp
‡Nagaoka University of Technology
Email: tsubone@vos.nagaokaut.ac.jp

Abstract—In this study, we consider drive-response of a coupled system of three dimensional piecewise-constant oscillators (PCOs). The oscillator consists of three linear capacitors, three voltage-controlled current sources with signum characteristics, and a rectifier diode. We construct a simple drive-response system of 3-D PCOs with master-slave couplings. We confirmed that the system exhibited chaotic generalized synchronization. In this paper, we discuss the chaotic generalized synchronization of piecewise-constant systems and confirm typical phenomena by laboratory experiments and rigorous solutions.

1. Introduction

Coupled oscillators are good models to explain complex nonlinear phenomena of nature and society. Chaotic synchronization [1] is an interesting problem for various fields such as physical, biological, and electrical engineering. Many reports of the synchronization of coupled chaotic systems have been released. Such synchronization includes some concepts such as complete synchronization $X_2(t) = X_1(t)$, lag synchronization $X_2(t) = X_1(t+\tau)$, and generalized synchronization $X_2(t) = G[X_1(t)]$, where X_1 and X_2 mean state variables of coupled oscillators. In this study, we will focus on generalized synchronization. In previous works, same interesting discussions have been provided by using numerical analysis and electrical circuit experiments [2, 3]. However the analysis often are difficult, because its complex behaviors. Then we consider a coupled system of third order piecewise-constant oscillators (3-D PCOs) [4]. Piecewise-constant oscillator is a simple switched dynamical system, and it exhibits some interesting nonlinear phenomena. The system can be analyzed by using rigorous solutions, because the dynamics is dominated by piecewise-constant vector fields. We observed generalized chaotic synchronization of the proposed system in laboratory, and confirmed the appropriateness by rigorous solutions. In this paper, we provide more detailed analysis and consider the bifurcations. In the Sec. 2, we explain the 3-D PCO. In Sec. 3, the drive-response coupled system of 3-D PCOs is represented. In Sec. 4, we show typical results of laboratory measurements and rigorous solutions. This paper is concluded in Sec. 5.

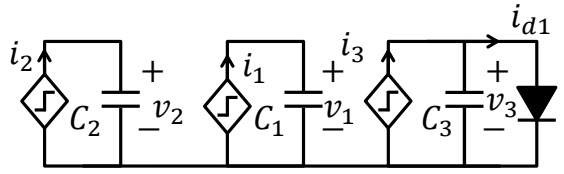

Figure 1: Block diagram of 3-d Piecewise-Constant Oscillator.

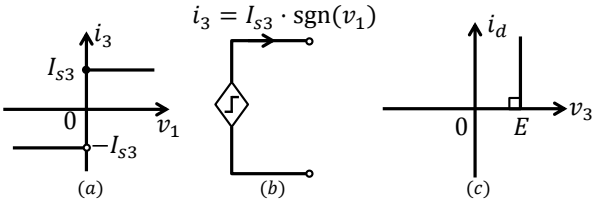

Figure 2: The symbol and characteristics.

2. 3-D piecewise-constant oscillator with a diode

In this section, we explain a 3-D piecewise-constant oscillator with a diode, and show typical behaviors on phase space. The block diagram of the system is shown in Fig. 1. The oscillator consists of three capacitors, three voltage-controlled current sources (VCCSs) with signum characteristics as shown in Fig. 2(a), and a rectifier diode which has an ideal characteristic as shown in Fig. 2(c). The dynamics of the system is described by two differential equations and idealized switching of the diode. When the diode is ON ($i_d = I_{s3} \cdot \mathrm{sgn}(v_1) > 0$), the dynamics is represented as follows,

$$\begin{cases} C_1 \dfrac{dv_1}{dt} &= I_{s1} \cdot \mathrm{sgn}(v_2 - E), \\ C_2 \dfrac{dv_2}{dt} &= I_{s2} \cdot \mathrm{sgn}(v_2 - v_1), \\ v_3 &= E, \end{cases} \tag{1}$$

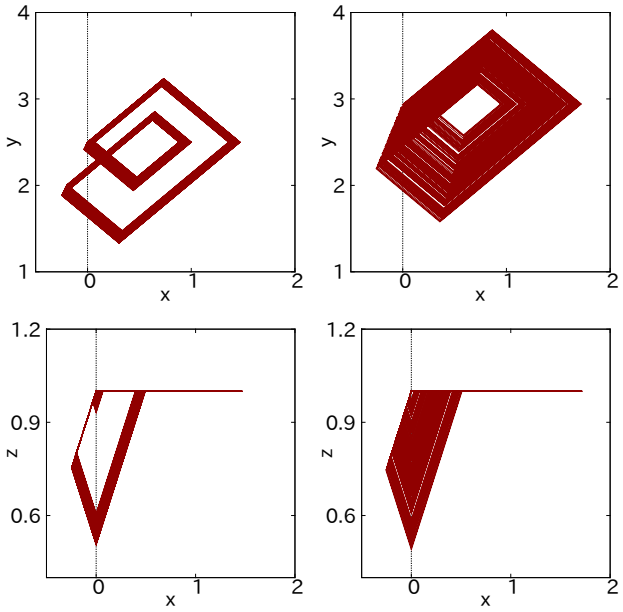

(a)$a = 4.4, b = 0.4$ (b)$a = 4.4, b = 0.34$

Figure 3: Typical attractors.

and when the diode is OFF ($v_3 < E$), the dynamics is as follows,

$$\begin{cases} C_1 \dfrac{dv_1}{dt} &= I_{s1} \cdot \mathrm{sgn}(v_2 - v_3), \\ C_2 \dfrac{dv_2}{dt} &= I_{s2} \cdot \mathrm{sgn}(v_2 - v_1), \\ C_3 \dfrac{dv_3}{dt} &= I_{s3} \cdot \mathrm{sgn}(v_1). \end{cases} \tag{2}$$

The dynamics (1) and (2) are rewritable as follows,

$$\begin{cases} \dot{x} &= \mathrm{sgn}(by - 1), \\ \dot{y} &= \mathrm{sgn}(y - ax), \\ z &= 1, \end{cases} \tag{3}$$

$$\begin{cases} \dot{x} &= \mathrm{sgn}(by - z), \\ \dot{y} &= \mathrm{sgn}(y - ax), \\ \dot{z} &= \mathrm{sgn}(x), \end{cases} \tag{4}$$

by using following normalized variables and dimensionless parameters.

$$\begin{gathered} a = \frac{C_2 I_{s1}}{C_1 I_{s2}},\ b = \frac{C_3 I_{s2}}{C_2 I_{s3}},\ \tau = \frac{I_{s3}}{C_3 E} t,\ \dot{x} = \frac{\mathrm{d}}{\mathrm{d}\tau} x, \\ x = \frac{C_1 I_{s3}}{C_3 I_{s1}} \frac{1}{E} v_1,\ y = \frac{C_2 I_{s3}}{C_3 I_{s2}} \frac{1}{E} v_2,\ z = \frac{1}{E} v_3. \end{gathered} \tag{5}$$

The switching condition is also renewed as follows, if $z = 1$, then OFF(4) $\rightarrow$ ON(3), and if $x = 0$, then ON(3) $\rightarrow$ OFF(4). Typical behavior of 3-D PCO is shown in Fig. 3. Some chaotic attractors are observed.

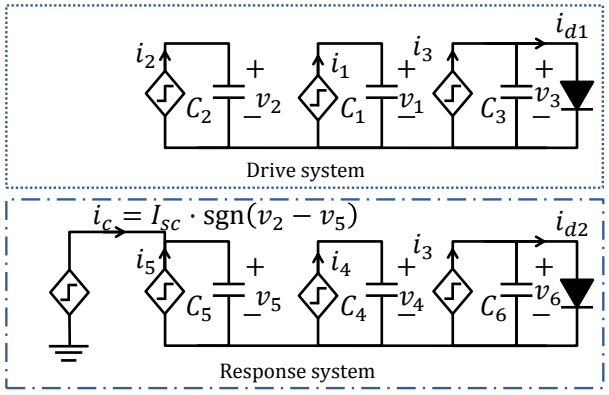

Figure 4: Coupled system block diagram.

3. A drive-response coupled system of 3-D PCOs

In this section, we explain a drive-response coupled system of 3-D PCOs. The block diagram is shown in Fig. 4. The upper circuit is a drive system, and the lower circuit is a response system.

The coupling factor i_c is given by difference between v_2 and v_5,

$$i_c = I_{sc} \cdot \mathrm{sgn}(v_2 - v_5). \tag{6}$$

The normalized differential equations of the coupled system are represented as follows,

$$\begin{cases} \dot{x_d} &= \mathrm{sgn}(b_d y_d - 1), \\ \dot{y_d} &= \mathrm{sgn}(y_d - a_d x_d), \\ z_d &= 1, \end{cases} \tag{7}$$

$$\begin{cases} \dot{x_d} &= \mathrm{sgn}(b_d y_d - z_d), \\ \dot{y_d} &= \mathrm{sgn}(y_d - a_d x_d), \\ \dot{z_d} &= \mathrm{sgn}(x_d). \end{cases} \tag{8}$$

$$\begin{cases} \dot{x_r} &= \mathrm{sgn}(b_r y_r - 1), \\ \dot{y_r} &= \mathrm{sgn}(y_r - a_r x_r) + \varepsilon \cdot \mathrm{sgn}(y_d - \gamma y_r), \\ z_r &= 1, \end{cases} \tag{9}$$

$$\begin{cases} \dot{x_r} &= \mathrm{sgn}(b_r y_r - z_r), \\ \dot{y_r} &= \mathrm{sgn}(y_r - a_r x_r) + \varepsilon \cdot \mathrm{sgn}(y_d - \gamma y_r), \\ \dot{z_r} &= \mathrm{sgn}(x_r). \end{cases} \tag{10}$$

a_d, b_d, a_r and b_r are circuit parameters of each systems, γ is

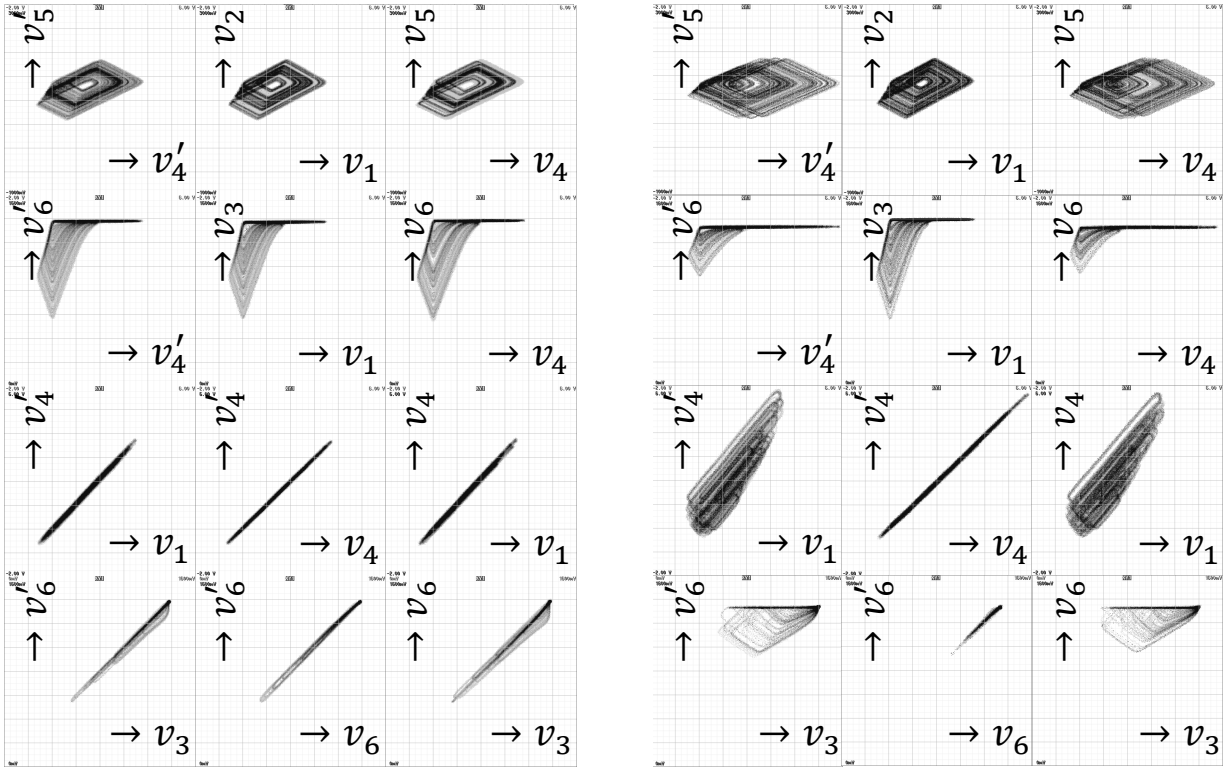

(a)A lower parameter mismatch (b)A higher parameter mismatch

Figure 5: The phase portrait of laboratory measurements. 1st row: horizontal division [1V], vertical division [0.5V]. 2nd row: horizontal division [1V], vertical division [0.2V]. 3rd row: horizontal division [1V], vertical division [1V]. 4th row: horizontal division [0.2V], vertical division [0.2V].

a ratio of coupled elements, and ε is a coupling strength.

$$\begin{aligned}
\tau &= \sqrt{\frac{I_{s6}I_{s3}}{C_3C_6E}}t,\ x_d = \sqrt{\frac{C_1^2I_{s3}I_{s6}}{C_3C_6I_{s1}^2}}\frac{1}{E}v_1,\\
y_d &= \sqrt{\frac{C_2^2I_{s3}I_{s6}}{C_3C_6I_{s2}^2}}\frac{1}{E}v_2,\ z_d = \sqrt{\frac{C_3I_{s6}}{C_6I_{s3}}}\frac{1}{E}v_3,\\
x_r &= \sqrt{\frac{C_4^2I_{s3}I_{s6}}{C_3C_6I_{s4}^2}}\frac{1}{E}v_4,\ y_r = \sqrt{\frac{C_5^2I_{s3}I_{s6}}{C_3C_6I_{s5}^2}}\frac{1}{E}v_5,\\
z_r &= \sqrt{\frac{C_6I_{s3}}{C_3I_{s6}}}\frac{1}{E}v_6,\ a_d = \frac{C_2I_{s1}}{C_1I_{s2}},\ b_d = \frac{C_3I_{s2}}{C_2I_{s3}},\\
a_r &= \frac{C_5I_{s4}}{C_4I_{s5}},\ b_r = \frac{C_6I_{s5}}{C_5I_{s6}},\ \gamma = \frac{C_2I_{s5}}{C_5I_{s2}},\ \varepsilon = \frac{I_{sc}}{I_{s5}}.
\end{aligned} \tag{11}$$

Switching condition of each systems differential equations are also renewed as follows, for drive system if $z_d = 1$, then OFF(8) $\rightarrow$ ON(7), and if $x_d = 0$, then ON(7)$\rightarrow$ OFF (8), and for response system, if $z_r = 1$, then OFF(10)$\rightarrow$ ON(9), and if $x_r = 0$, then ON(9)$\rightarrow$ OFF(10). The coupled system exhibits the complete synchronization if the parameter condition satisfies follows,

$$a_d = a_r, b_d = d_r, \gamma = 1, \varepsilon >> 1. \tag{12}$$

4. Circuit experiments and rigorous solution

In this section, in order to consider chaotic generalized synchronizations, we prepare a second response system. The construction and parameters of the 2nd response system are same as 1st one, but thier initial conditions are different. The parameters of the 1st and 2nd response system are $a_r' \approx a_r, b_r' \approx b_r, \gamma' \approx \gamma$, and $\varepsilon' \approx \varepsilon$. If the drive-response system exhibits the complete synchronization, 1st and 2nd response systems also synchronize completely. In the laboratory measurements, we observed two cases depended on the parameter mismatch between b_r and b_d:

1. All response systems are synchronized, that is complete synchronization.

2. The 1st and 2nd response systems are synchronized, but the drive system is not synchronized, that is generalized synchronization.

In the case where parameter mismatch is sufficiently small, we can observe experimental measurements as shown in Fig. 5(a). In the case where parameter mismatch is relatively large, we also observe attractors as shown in Fig. 5(b). The coupled states y_d and y_r are synchronized regardless of the magnitude of the parameter mismatch. The

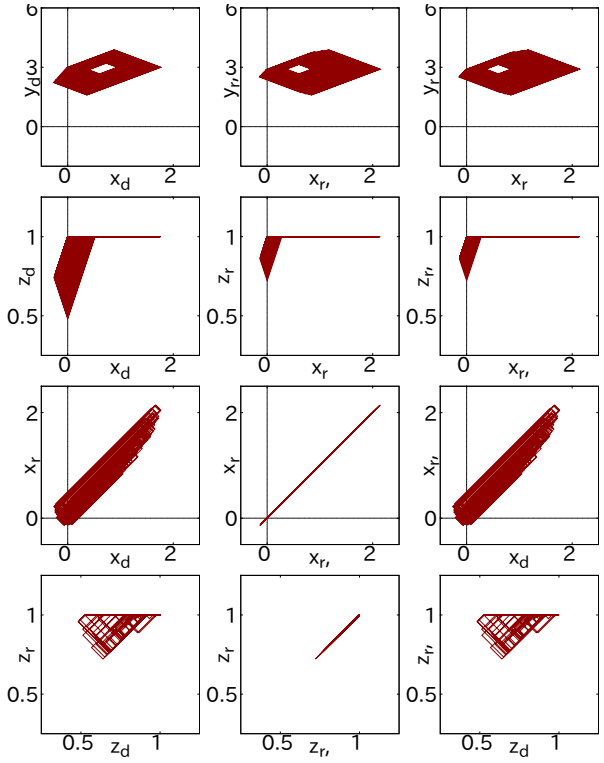

Figure 6: Rigorous solution. The parameters are $a_d = 4.4, b_d = 0.3334, b_r = 0.3444$.

phase portraits of rigorous solution are shown in Fig. 6. The results are qualitatively consistent with the Fig. 5(b).

We confirmed the transition of the synchronization relate to the parameter mismatch between the drive system and both response systems, by using the cross-correlation coefficients.

$$C_{xdr} = \frac{\sum_{i=0}^{M}(x_{di} - \bar{x_d})(x_{ri} - \bar{x_r})}{\sqrt{\sum_{i=0}^{M}(x_{di} - \bar{v_d})^2 \sum_{i=0}^{M}(x_{ri} - \bar{x_r})^2}}. \qquad (13)$$

The cross-correlation coefficients of 1st response system versus the drive system (C_{xdr}, C_{zdr}) and 2nd response system (C_{xrr}, C_{zrr}) are represented in Fig. 7. If the parameter mismatch is small, both response systems are synchronized. By increasing the parameter mismatch, the correlation coefficients of 1st response system versus the drive system decreasing, but one of both response systems does not decreased until $b_r = 0.353$. It is generalized synchronization. If the parameter mismatch is further increased, it goes to asynchronous.

5. Conclusion

We consider drive-response system with 3-D piecewise-constant oscillators. On the laboratory measurements and rigorous solutions, the proposed system are observed to exhibit the synchronization phenomena when coupling

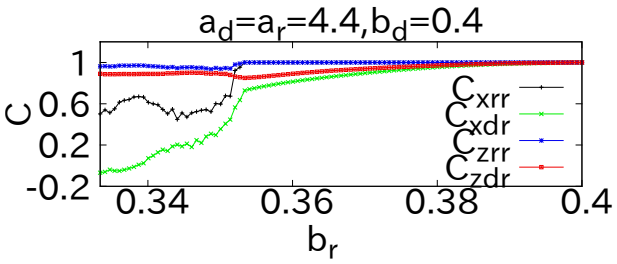

Figure 7: One-parameter bifurcation diagram. Horizontal: the parameter of the 1st response system b_r, vertical: cross-correlation coefficients.

strength is sufficient stronger. We observed transition of cross-correlation coefficients with increasing the parameter mismatch between drive and response systems. Therefore, we confirmed bifurcation to the asynchronous via the generalized synchronization from the complete synchronization. In the future, we will analysis using the Lyapunov exponent.

References

[1] L. M. Pecora and T. L. Carroll, "Synchronization in Chaotic Systems," Phys. Rev. Lett., vol. 64, No. 8, pp.921-824, 1990.

[2] A. Kittel, J. Parisi and K. Pyragas, "Generalized synchronization of in electronic circuit experiments," Physica D, vol.112, pp.459-471, 1998.

[3] K. Mitsubori and K. Ebisawa, "Gnereralized Synchronization of Chaos in Unidirectionally and Nutually Coupled Four Shinriki's Circuits," IEICE Trans. A, vol. J94-A, No. 8, pp. 587-595, 2011.

[4] T. Tsubone and T. Saito, "On a Basic Piecewise-Constant system," Proc. IEEE/ISCAS, vol.I, pp.248-251, 2000.